J Math Chem (2015) 53:1997–2017
DOI 10.1007/s10910-015-0531-5

ORIGINAL PAPER

Solving the adsorption integral equation with Langmuir-kernel and the influence of temperature on the stability of the solution

Steffen Arnrich[1] · **Peter Bräuer**[1] · **Grit Kalies**[1]

Received: 3 March 2015 / Accepted: 29 June 2015 / Published online: 11 July 2015

Abstract Adsorption energy distribution functions can be calculated from measured adsorption isotherms by solving the adsorption integral equation. In this context, it is common practice to use general regularization methods, which are independent of the kernel of the adsorption integral equation, but do not permit error estimation. In order to overcome this disadvantage, we present in this paper a solution theory which is tailor-made for the Langmuir kernel of the adsorption integral equation. The presented theory by means of differentiation and Fourier series is the basis for a regularization method with explicit terms for error amplification. By means of simple and complicated adsorption energy distribution functions we show for ideal gas adsorption isotherms without measurement error that reliable distribution functions can be obtained from the isotherms. Furthermore we show how the stability of the solution depends on temperature.

Keywords Adsorption isotherms · Adsorption energy distribution · Adsorption integral equation · Regularization · Temperature dependence

Mathematics Subject Classification 45

1 Introduction

For more than fifty years, significant efforts have been made for describing experimental gas adsorption on solids by lattice models [1–5]. The consideration of the local

✉ Steffen Arnrich
arnrich@htw-dresden.de

[1] Department of Mechanical Engineering/Process Engineering, University of Applied Sciences Dresden (HTW), Friedrich-List-Platz 1, 01069 Dresden, Germany

surface coverage θ_l at adsorption sites of the same type of molar adsorption energy u leads to the adsorption integral equation

$$\theta_t(p) = \int_{u_{\min}}^{u_{\max}} \theta_l(p,u)\ F(u)\ \mathrm{d}u, \quad 0 \le p < \infty \qquad T = \text{const.} \tag{1}$$

with the measured total isotherm $\theta_t = \theta_t(p)$, the local isotherm $\theta_l = \theta_l(p,u)$, the gas pressure p, and the molar energy u released by adsorption with the minimal and maximal values $u_{\min}$ and $u_{\max}$. The searched adsorption energy distribution function F that is called in this paper AED is restricted by $F \ge 0$ and the normalization condition $\int_{u_{\min}}^{u_{\max}} F(u)\ \mathrm{d}u = 1$.

For the local isotherm θ_l, a suitable model has to be applied. Since for calculating AEDs, only the very low pressure ranges of measured adsorption isotherms are analyzed, it makes sense to use the Langmuir equation $\theta_l = K_L p/(1 + K_L p)$ with $K_L = K_L(T,u)$ for localized monolayer adsorption as the model for the local isotherm.

With $y = K_0(T)\ p$ and the statistical-thermodynamic expression for the Langmuir constant $K_L = K_0(T)\ \exp\left(\frac{u}{RT}\right)$ [2], the integral Eq. (1) turns into the following general form with Langmuir kernel:

$$f(y) = \int_{u_{\min}}^{u_{\max}} \frac{y \exp\left(\frac{u}{RT}\right)}{1 + y \exp\left(\frac{u}{RT}\right)} F(u)\,\mathrm{d}u, \qquad 0 \le y < \infty, \tag{2}$$

where $f(y) = \theta_t(p)$. Because of the simple relation between θ_t and f we call f also the total isotherm.

Equations (1) and (2) as Fredholm integral equations of the first kind are ill-posed and in particular unstable problems if the integration interval is finite [6]. Such unstable problems can be solved by two strategies: (a) restoring stability by changing the setting, and (b) regularization.

In [7,8] we have shown that strategy (a) is often inapplicable although numerous so-called analytical or ansatz methods for solving (2) exist. In this paper, we show that restoring stability by changing the setting is impossible for Eq. (2) unless one restricts the set of possible AEDs to a set of functions that can be described by finitely many parameters. For the analytical or ansatz methods, the chosen restrictions have to be justified by a priori information. Otherwise these methods can produce untrustworthy results.

In general, if there are no unnatural restrictions to the set of AEDs, regularization [6,9–11] is the method of choice. However, for estimating the difference between true and calculated AEDs, additional assumptions are required being justified by a priori information. A regularization scheme can never converge uniformly, i.e. the quality of approximation is not independent of the total isotherm f. Therefore, every regularization scheme has its limitations, too. In order to make trustworthy statements about the quality of approximation for the calculated AED, these limitations must be

known. Up to now, none of the suggested procedures for solving (1) has prevailed [1–5].

In this paper, we present the basis for a further regularization scheme. While other schemes are constructed independent of the kernel, our scheme is tailor-made for the Langmuir kernel. The objective of our work is to establish a regularization scheme fulfilling the following requirements:

I. There are explicit terms for error amplification.
II. There is a simple criterion to characterize the quality of approximation.

Amongst other things, these requirements will help to find the optimal regularization parameter. Whereas in general, it remains unclear which a priori information is needed, item II can deliver the needed information.

The paper is structured as follows. After discussing the general strategies for a stable approximate solution of ill-posed problems in Sect. 2, we derive in Sect. 3 inversion formulas for (2) basing on a transformation related to the Stieltjes transformation. In Sect. 4, we apply these formulas and derive two suitable candidates for a regularization scheme. In Sect. 5, the relation between temperature and stability is investigated. Finally in Sect. 6, the results are summarized.

2 Ill-posed problems

According to Hadamard [12], a problem is called well-posed if it satisfies the following conditions:

(i) A solution exists.
(ii) The solution is unique.
(iii) The solution depends continuously on the data (stability).

Otherwise the problem is called ill-posed.

As item (iii) is rather vague, a concept is required, which is suitable for integral equations with restrictions, for defining well-posedness and especially stability for a setting.

Inspired by [6] and [10], we define ill-posed problems as follows:

Definition Let A:$M \rightarrow N$ be a mapping between the metric spaces (M, d_M) and (N, d_N). We call the problem [A, (M, d_M), (N, d_N)] well-posed if A is bijective and the inverse mapping A^{-1} is hölder continuous. Otherwise we call the problem ill-posed.

In most applications—as in our case—the mapping A is injective but $\mathrm{A}^{-1} : \mathrm{A}(M) \rightarrow M$ is not hölder continuous. We call that the unstable case.

As already mentioned in the introduction, one strategy to turn an ill-posed problem in a well-posed one is to change the setting, that means to change the metric spaces (M, d_M) and (N, d_N). This is often impossible because the choice of setting is dictated by practical needs. Usually in the context of integral equations, M is the set of all functions of interest. N has to be chosen large enough in order to find simple approximations for the functions in $\mathrm{A}(M)$ being often complicated. The metrics are the main problem. In general, they should measure the distance between non-smooth functions because the perturbations are non-smooth due to the measuring process.

The second strategy dealing with unstable problems, the method of regularization, leaves the metrics unchanged. The main idea is here the construction of stable, i.e. hölder continuous mappings $\mathrm{B}_\lambda : N \to M$, $0 < \lambda$ with the *property of pointwise convergence* [6]

$$\lim_{\lambda \to 0} \mathrm{B}_\lambda A\psi = \psi \tag{3}$$

for all $\psi \in M$. The parameter λ is called the *regularization parameter.* For erroneous data g_ε of $g \in \mathrm{A}(M)$ with $d_N(g_\varepsilon, g) \leq \varepsilon$, we consider every $\mathrm{B}_\lambda g_\varepsilon$ as approximation of the solution of $\mathrm{A}\psi = g$. In order to achieve an acceptable error $d_M(\mathrm{B}_\lambda g_\varepsilon, \psi)$ for the approximate solution, we need a choice of λ depending on the error level ε and the data g_ε. A mapping $\gamma : (0, \infty) \times N \to (0, \infty)$ is called choice of the parameter λ if

$$\lim_{\varepsilon \to 0} d_M(\mathrm{B}_{\gamma(\varepsilon, g_\varepsilon)} g_\varepsilon, \mathrm{A}^{-1} g) = 0 \tag{4}$$

does hold for all $g \in \mathrm{A}(M)$ and $g_\varepsilon \in N$ with $d_N(g_\epsilon, g) \leq \varepsilon$.

Any pair $(\{\mathrm{B}_\lambda\}_{\lambda>0}, \gamma)$ fulfilling (3) and (4) is called a *regularization* or *regularization scheme* for the problem [A, (M, d_M), (N, d_N)] [10].

Our main purpose in this article is the construction of families $\{\mathrm{B}_\lambda\}_{\lambda>0}$ with the property of pointwise convergence (3) as a basis for a regularization scheme for Eq. (2).

Remark Since we are dealing with integral equations, we suppose that $M - M$ and $N - N$ belong to any function spaces X or Y, resp., and that the metrics d_M and d_N are induced by norms on these spaces.

3 Inversion formulas

In this section after a suitable change of variables, we derive inversion formulas for (2). These formulas are the basis for constructing the families $\{\mathrm{B}_\lambda\}_{\lambda>0}$. Furthermore, we show that (2) cannot be stabilized by changing the setting unless one restricts strongly the set of admissible F.[1]

3.1 Change of variables

In [7,8] we derived an inversion formula for (2) by means of Stieltjes transformation:

$$F(u) = \lim_{\eta \downarrow 0} \frac{f\left(\frac{1}{-\exp(\frac{u}{RT}) - i\eta}\right) - f\left(\frac{1}{-\exp(\frac{u}{RT}) + i\eta}\right)}{2\pi RTi}, \qquad u_{\min} < u < u_{\max}, \tag{5}$$

which holds for continuous adsorption energy distributions (i denotes the imaginary unit).

In order to apply (5), the total isotherm has to be available in analytical form. If no special form of F is assumed, there is no constructive way to obtain a useful simple

[1] In the following whenever it is necessary, F is continued by 0 outside of $[u_{\min}, u_{\max}]$.

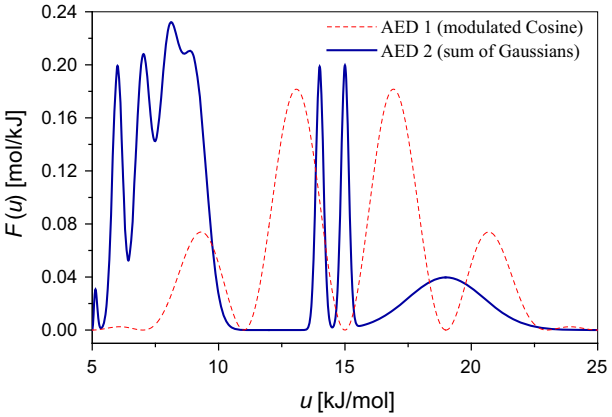

Fig. 1 Synthetic adsorption energy distribution functions (AEDs)

approximation (ansatz) for f by means of measured data. In [7,8], we have shown that none of the common ansatzes can be used. For that reason, there is a need to derive formulas of practical use. The first step is the following change of variables:

$$y = \exp\left(-\frac{\zeta}{RT}\right) \qquad \text{or} \qquad \zeta = -RT \ln y \tag{6}$$

leading to the transformed total isotherms φ:

$$\begin{aligned}\varphi(\zeta) := f\left(\exp\left(-\frac{\zeta}{RT}\right)\right) &= \int_{u_{\min}}^{u_{\max}} \frac{\exp\left(\frac{u-\zeta}{RT}\right)}{1+\exp\left(\frac{u-\zeta}{RT}\right)} F(u)\,\mathrm{d}u \\ &= \int_{u_{\min}}^{u_{\max}} \frac{F(u)}{1+\exp\left(\frac{\zeta-u}{RT}\right)}\mathrm{d}u, \qquad \zeta \in \mathbb{R}\end{aligned} \tag{7}$$

In the following, we will illustrate (7) by means of examples used in this paper. Figure 1 shows two synthetic adsorption energy distributions F (AEDs): a simple AED generated by modulated cosine, and a more complicated AED obtained by a sum of Gaussians.

The corresponding total isotherms f and transformed total isotherms φ calculated from AED 1 and AED 2 according to (7) are presented in Fig. 2.

Equation (7) is a convolution integral equation with the convolution kernel

$$k = k(t) = \frac{1}{1+\exp\left(\frac{t}{RT}\right)}, \qquad t \in \mathbb{R}. \tag{8}$$

3.2 Complex inversion formulas

A deconvolution of (7) using the complex arguments $\zeta + i\alpha$ is based on the fact that the sequence of functions

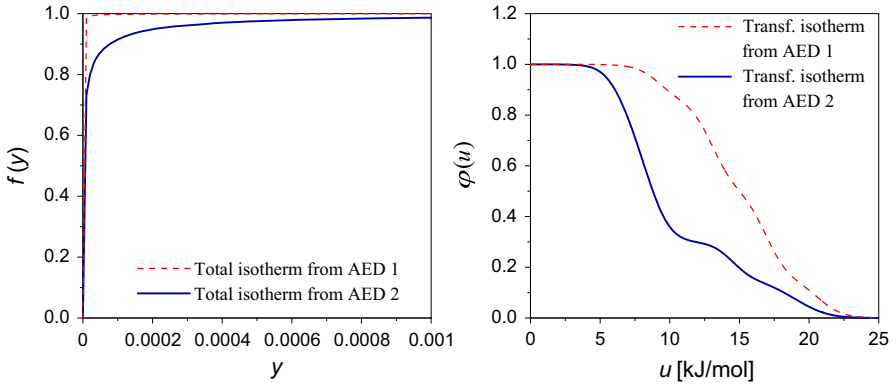

Fig. 2 *Left* Total gas adsorption isotherms for $T = 77$ K with $f(y) = \Theta_t(p)$; $y = K_0(T)\,p$ (K_0 was normed to 1 Pa^{-1}). *Right* Corresponding transformed total gas adsorption isotherms for $T = 77$ K

$$\begin{aligned}\delta_\alpha(t) &:= \frac{k(t - i\alpha) - k(t + i\alpha)}{2i\alpha} \\ &= \frac{1}{\alpha}\,\frac{\sin\frac{\alpha}{RT}}{2\cosh\frac{t}{RT} + 2\cos\frac{\alpha}{RT}}, \qquad t \in \mathbb{R},\ 0 \le \alpha < \pi RT \end{aligned} \tag{9}$$

is a Dirac-sequence. In order to see this, we use

$$\int_a^b \delta_\alpha(t)\,\mathrm{d}t = \frac{RT}{\alpha}\arctan\left(\frac{\exp\left(\frac{t}{RT}\right) + \cos\frac{\alpha}{RT}}{\sin\frac{\alpha}{RT}}\right)\Bigg|_a^b$$

and obtain

a)

$$\int_{-\infty}^{\infty} \delta_\alpha(t)\,\mathrm{d}t = \frac{RT}{\alpha}\left[\frac{\pi}{2} - \arctan\left(\cot\frac{\alpha}{RT}\right)\right] = \frac{RT}{\alpha}\left[\frac{\pi}{2} - \frac{\pi}{2} + \frac{\alpha}{RT}\right] = 1,$$

b)

$$\begin{aligned}\lim_{\alpha\uparrow\pi RT}\int_{-\infty}^{-r} \delta_\alpha(t)\,\mathrm{d}t &= \lim_{\alpha\uparrow\pi RT}\frac{RT}{\alpha}\left[\arctan\left(\frac{\exp\left(\frac{-r}{RT}\right) + \cos\frac{\alpha}{RT}}{\sin\frac{\alpha}{RT}}\right) - \frac{\pi}{2} + \frac{\alpha}{RT}\right] \\ &= \pi\left[-\frac{\pi}{2} - \frac{\pi}{2} + \pi\right] = 0,\ r > 0,\end{aligned}$$

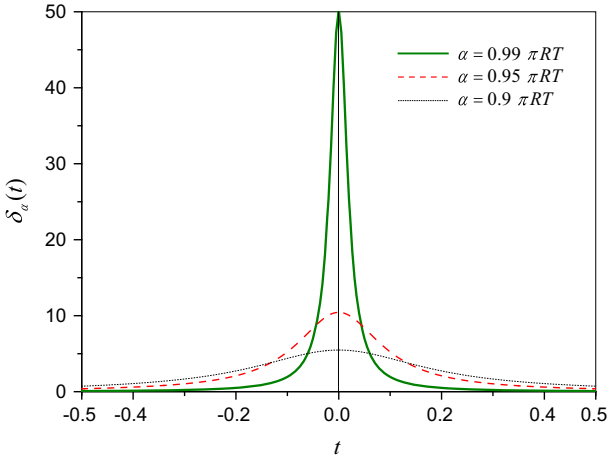

Fig. 3 The functions δ_α for different values of α and $T = 77$ K

c)

$$\lim_{\alpha\uparrow\pi RT}\int_r^\infty \delta_\alpha(t)\,\mathrm{d}t = \lim_{\alpha\uparrow\pi RT}\frac{RT}{\alpha}\left[\frac{\pi}{2} - \arctan\left(\frac{\exp\left(\frac{r}{RT}\right)+\cos\frac{\alpha}{RT}}{\sin\frac{\alpha}{RT}}\right)\right]$$
$$= \pi\left[\frac{\pi}{2}-\frac{\pi}{2}\right] = 0,\ r > 0.$$

(a), (b) and (c) yield the assertion [13].

In Fig. 3, δ_α is shown for three different values of α.

Let us now define the functions

$$F_\alpha(\zeta) := \frac{\varphi\,(\zeta - i\alpha) - \varphi\,(\zeta + i\alpha)}{2i\alpha} = \int_{u_{\min}}^{u_{\max}} F(u)\,\frac{k\,(\zeta - u - i\alpha) - k\,(\zeta - u + i\alpha)}{2i\alpha}\,\mathrm{d}u$$
$$= \int_{u_{\min}}^{u_{\max}} F(u)\,\delta_\alpha(\zeta - u)\,\mathrm{d}u, \qquad \zeta \in \mathbb{R}. \tag{10}$$

Since $\delta_\alpha \geq 0$, $0 \leq \alpha < \pi RT$ is a Dirac sequence, we obtain for integrable F (see [13])

$$\lim_{\alpha\uparrow\pi RT} \|F - F_\alpha\|_{1;\mathbb{R}} = 0, \tag{11}$$

using the standard notation for integral norms. (11) can be improved under additional assumptions on F :

- If F is p-integrable for some $p \geq 1$, then yields

$$\lim_{\alpha\uparrow\pi RT} \|F - F_\alpha\|_{p;\mathbb{R}} = 0 \tag{12}$$

- If F is piecewise continuous, then follows by the symmetry of the δ_α

$$\lim_{\alpha \uparrow \pi RT} \frac{\varphi(u - i\alpha) - \varphi(u + i\alpha)}{2i\alpha} = \frac{F(u^+) + F(u^-)}{2} \tag{13}$$

where $F(u^+)$ and $F(u^-)$ denote the right-hand or left-hand limit, resp.

The inversion formulas (11) as well as (13) are not directly applicable because the same difficulties occur as by applying (5). However, they are the basis for real inversion formulas depending only on the knowledge of φ and its derivatives on the real axis.

3.3 Real inversion formulas

3.3.1 Derivation of the basic formula

A real inversion formula can be obtained by developing φ into a series. This is possible because the folding kernel k as defined in (8) is a holomorphic function in the complex stripe-domain $S := \{z = t + i\alpha |\ \ t \in \mathbb{R},\ \ |\alpha| < \pi RT\}$. Hence φ is holomorphic in S. From this follows

$$\varphi(z) = \sum_{k=0}^{\infty} \frac{\varphi^{(k)}(\xi)}{k!}(z - \xi)^k \text{ for all } \xi \in \mathbb{R},\ z \in \mathbb{C} \text{ with } |z - \xi| < \pi RT. \tag{14}$$

Therefore, we can develop F_α as defined in (10) into a series:

$$\begin{aligned} F_\alpha(\xi) = \frac{\varphi\ (\xi - i\alpha) - \varphi\ (\xi + i\alpha)}{2i\alpha} &= \frac{1}{2i\alpha} \sum_{k=0}^{\infty} \frac{(-i\alpha)^k - (i\alpha)^k}{k!} \varphi^{(k)}(\xi) \\ &= \frac{1}{\alpha} \sum_{k=0}^{\infty} \frac{(-1)^{k+1}\alpha^{2k+1}}{(2k+1)!} \varphi^{(2k+1)}(\xi). \end{aligned} \tag{15}$$

(11) yields then

$$\lim_{\alpha \uparrow \pi RT} \left\| F - \frac{1}{\alpha} \sum_{k=0}^{\infty} \frac{(-1)^{k+1}\alpha^{2k+1}}{(2k+1)!} \varphi^{(2k+1)} \right\|_{1;\mathbb{R}} = 0. \tag{16}$$

This result can be improved if F is square-integrable. Then it holds by (12)

$$\lim_{\alpha \uparrow \pi RT} \left\| F - \frac{1}{\alpha} \sum_{k=0}^{\infty} \frac{(-1)^{k+1}\alpha^{2k+1}}{(2k+1)!} \varphi^{(2k+1)} \right\|_{2;\mathbb{R}} = 0. \tag{17}$$

Since all $\varphi^{(2k+1)}$ are square-integrable, (17) can be written also as

$$\lim_{\alpha\uparrow\pi RT}\ \lim_{n\to\infty}\left\| F-\frac{1}{\alpha}\sum_{k=0}^{n}\frac{(-1)^{k+1}\alpha^{2k+1}}{(2k+1)!}\,\varphi^{(2k+1)}\right\|_{2;\mathbb{R}}=0. \tag{18}$$

In [14,15], it is shown that the limits in (18) can be interchanged.[2] It follows

$$0=\lim_{n\to\infty}\left\| F-\frac{1}{\pi RT}\sum_{k=0}^{n}\frac{(-1)^{k+1}(\pi RT)^{2k+1}}{(2k+1)!}\,\varphi^{(2k+1)}\right\|_{2;\mathbb{R}}. \tag{19}$$

Since F in (19) is zero outside of $[u_{\min},u_{\max}]$, the domain of integration can be replaced by $[u_{\min},u_{\max}]$.

3.3.2 Illustration of instability

By means of (19) we can illustrate the instability of the adsorption integral Eq. (2).

For adsorption energy distributions F_1 and F_2, by (19) we get

$$\begin{aligned}\|F_1-F_2\|_{2;I}&=\lim_{n\to\infty}\left\|\sum_{k=0}^{n}\frac{(-1)^{k+1}(\pi RT)^{2k}}{(2k+1)!}\left(\varphi_1^{(2k+1)}-\varphi_2^{(2k+1)}\right)\right\|_{2;I}\\&\le\sum_{k=0}^{\infty}\frac{(\pi RT)^{2k}}{(2k+1)!}\left\|\varphi_1^{(2k+1)}-\varphi_2^{(2k+1)}\right\|_{2;I},\quad I:=[u_{\min},u_{\max}]\end{aligned} \tag{20}$$

According to (20), information about the mean squares $\left\|\varphi_1^{(2k+1)}-\varphi_2^{(2k+1)}\right\|_{2;I}$ is required to estimate the mean square $\|F_1-F_2\|_{2;I}$. By measuring total isotherms, we can only estimate the mean square $\|\varphi_1-\varphi_2\|_{2;I}$, but do not have access to $\left\|\varphi_1^{(2k+1)}-\varphi_2^{(2k+1)}\right\|_{2;I}$, because numerical differentiation itself is unstable if only the mean square or maximal error is known. With increasing order of the derivative, $\left\|\varphi_1^{(2k+1)}-\varphi_2^{(2k+1)}\right\|_{2;I}$ becomes more unstable.

For stability, a norm $\|\cdot\|$ that measures $\|\varphi_1-\varphi_2\|$ on the one hand needs *to be controlled* by $\|\varphi_1-\varphi_2\|_{2;I}$ and on the other hand needs *to control* the right-hand side of (20). The only way to achieve stability is to restrict the set of admissible F. This restriction has to be done in such a way that the derivatives $\varphi^{(2k+1)}$ depend analytically on φ, for instance if any admissible F can be characterized by a parameter vector belonging to a given subset of $\mathbb{R}^n$. If this restriction cannot be justified by physical or chemical reasons, then the finding of an approximate solution of sufficient precision is a matter of chance.

[2] This is actually done for the Stieltjes transform but the proof can be done analogously for our case by using a simple change of variables that transforms (7) into a Stieltjes integral.

3.3.3 Derivation of weak formulas

Utilizing (19) as the basis of a regularization method, one has to keep in mind that only a few derivatives of φ can be taken into account. Naturally, this limits the accuracy of approximation. Furthermore, (19) contains no explicit terms for error amplification.

In order to overcome problems with numerical differentiation, (19) can be used to compute suitable scalar products $\int_{u_{\min}}^{u_{\max}} F(u)p(u)\,\mathrm{d}u$ for recalculating F. Our hope is to find explicit terms for error amplification (see Sect. 4) for the right choice of the functions p. As a first step, we compute the above scalar products for functions p satisfying general conditions.

Let p be a holomorphic function such that

$$p_{\max} = p_{\max}(u) := \max_{0\le\gamma\le 2\pi} \left| p\left(u + \pi RTe^{i\gamma}\right)\right|, \qquad u \in \mathbb{R} \tag{21}$$

is integrable on $\mathbb{R}$. Then by Cauchy's integral formula, all derivatives of p are integrable which implies

$$\lim_{u\to\pm\infty} p^{(k)}(u) = 0, \qquad k = 0, 1, 2, \ldots \tag{22}$$

Under these assumptions, we get

$$\int_{u_{\min}}^{u_{\max}} F(u)p(u)\,\mathrm{d}u = \lim_{n\to\infty} \int_{-\infty}^{\infty} \frac{1}{\pi RT} \sum_{k=0}^{n} \frac{(-1)^{k+1}(\pi RT)^{2k+1}}{(2k+1)!}\, \varphi^{(2k+1)}(u)p(u)\,\mathrm{d}u \tag{23}$$

$$= \int_{-\infty}^{\infty} \varphi(u) \frac{1}{\pi RT} \sum_{k=0}^{\infty} \frac{(-1)^{k}(\pi RT)^{2k+1}}{(2k+1)!}\, p^{(2k+1)}(u)\,\mathrm{d}u$$

$$= \int_{-\infty}^{\infty} \varphi(u) \frac{p(u+i\pi RT) - p(u-i\pi RT)}{2i\pi RT}\,\mathrm{d}u. \tag{24}$$

If p does not satisfy (21) but has at least polynomial growth, then we obtain by a similar computation

$$\int_{u_{\min}}^{u_{\max}} F(u)p(u)\,\mathrm{d}u = \int_{-\infty}^{\infty} \varphi'(u) \frac{P(u-i\pi RT) - P(u+i\pi RT)}{2i\pi RT}\,\mathrm{d}u \tag{25}$$

where P is an antiderivative of p.

We call (24) and (25) weak inversion formulas.

4 Application of the formulas and numerical examples

In the following, we want to apply and compare the basic inversion formula (19) and the two weak inversion formulas (24) and (25). Furthermore, we show the influence of numerical differentiation on the accuracy of recalculated AEDs. Throughout the rest of the paper, we suppose that the AEDs are at least square-integrable.

4.1 Foldings and differentiation

We start with an application of (37) that can be considered as an analogon to (31). For this purpose, we use the fact that F can be approximated by foldings with Gaussians:

$$g_\sigma(u) = \frac{1}{\sqrt{2\pi}\sigma} \exp\left(-\frac{u^2}{2\sigma^2}\right), \qquad \sigma > 0.$$

Since the Gaussians are holomorphic satisfying (21), we obtain by applying (24) to $p = g(u - \cdot)$:

$$F(u) = \operatorname*{l.i.m.}_{\sigma \downarrow 0} \int_{-\infty}^{\infty} \varphi(v) \frac{g_\sigma(u - v - i\pi RT) - g_\sigma(u - v + i\pi RT)}{2i\pi RT} \mathrm{d}v, \tag{26}$$

where l.i.m. stands for "limes in medio" and indicates the limit in mean square.

Now we have

$$\begin{aligned}
&\frac{g_\sigma(t - i\pi RT) - g_\sigma(t + i\pi RT)}{2i\pi RT} \\
&= \frac{1}{\sqrt{2\pi}\sigma} \frac{\exp\left(-\frac{(t-i\pi RT)^2}{2\sigma^2}\right) - \exp\left(-\frac{(t+i\pi RT)^2}{2\sigma^2}\right)}{2i\pi RT} \\
&= \frac{\exp\left(-\frac{t^2}{2\sigma^2}\right)}{\sqrt{2\pi}\sigma} \frac{\exp\left(\frac{it\pi RT}{\sigma^2}\right) - \exp\left(-\frac{it\pi RT)^2}{\sigma^2}\right)}{2i\pi RT} \exp\left(\frac{(\pi RT)^2}{2\sigma^2}\right) \\
&= \exp\left(\frac{(\pi RT)^2}{2\sigma^2}\right) \frac{\sin\left(\frac{\pi RTt}{\sigma^2}\right)}{\pi RT} g_\sigma(t).
\end{aligned}$$

Inserting the above result for $t = u - v$ into (26), yields

$$F(u) = \operatorname*{l.i.m.}_{\sigma \downarrow 0} \exp\left(\frac{(\pi RT)^2}{2\sigma^2}\right) \int_{-\infty}^{\infty} \varphi(v) \frac{\sin\left(\frac{\pi RT(u-v)}{\sigma^2}\right)}{\pi RT} g_\sigma(u - v)\, \mathrm{d}v. \tag{27}$$

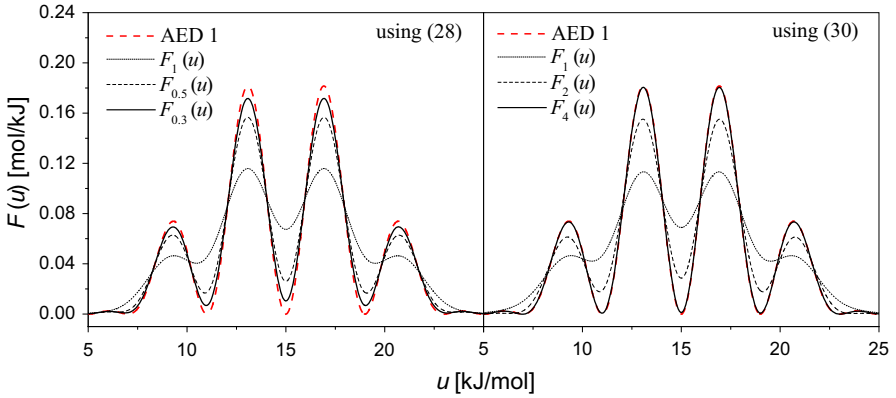

Fig. 4 Original synthetic AED 1 compared with recalculations by means of (28) for $\sigma = 1,\ \sigma = 0.5,\ \sigma = 0.3$ (numerically, $\sigma = 0.3$ is the smallest possible value) and (30) for $n = 1,\ n = 2,\ n = 4$ and $T = 77$ K

Choosing

$$F_\sigma(u) := \exp\left(\frac{(\pi RT)^2}{2\sigma^2}\right) \int_{-\infty}^{\infty} \varphi(v) \frac{\sin\left(\frac{\pi RT(u-v)}{\sigma^2}\right)}{\pi RT} g_\sigma(u-v)\,\mathrm{d}v \tag{28}$$

as an approximation of F, we see that the amplitude of an error in φ will be amplified by the factor $\exp\left(\frac{(\pi RT)^2}{2\sigma^2}\right)$.

The sinus-term reflects the differentiation process which leads to an additional amplification of error. The parameter σ can be considered as an analogue to the increment for numerical differentiation. This can be seen by considering (23). It becomes clear that (40) is identical with

$$F(u) = \underset{\sigma \downarrow 0}{\text{l.i.m.}}\ \underset{n\to\infty}{\text{l.i.m.}} \frac{1}{\pi RT} \sum_{k=0}^{n} \frac{(-1)^{k+1}(\pi RT)^{2k+1}}{(2k+1)!} \varphi_\sigma^{(2k+1)}(u) \tag{29}$$

where $\varphi_\sigma^{(2k+1)}(u) := \int_{-\infty}^{\infty} \varphi^{(2k+1)}(v) g_\sigma(u-v)\,\mathrm{d}v$ is an approximation of $\varphi^{(2k+1)}$.

Hence we can suppose that the approximations F_σ and

$$F_n(u) := \frac{1}{\pi RT} \sum_{k=0}^{n} \frac{(-1)^{k+1}(\pi RT)^{2k+1}}{(2k+1)!} \varphi^{(2k+1)}(u) \tag{30}$$

yield similar results.

In Figs. 4, 5, the recalculated adsorption energy distribution functions F by means of the approximations (28) and (29) are compared with the original distributions AED 1 and 2 as shown in Fig. 1.

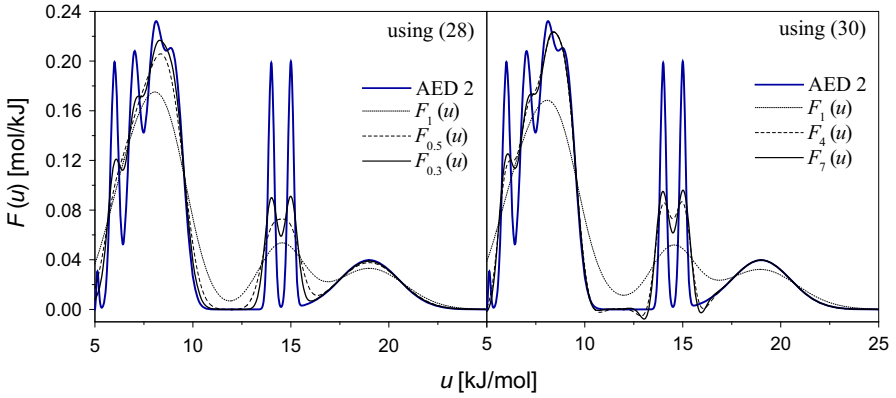

Fig. 5 Original synthetic AED 2 compared with recalculations by means of (28) for $\sigma = 1,\ \sigma = 0.5,\ \sigma = 0.3$ (numerically, $\sigma = 0.3$ is the smallest possible value) and (30) for $n = 1,\ n = 4,\ n = 7$ and $T = 77$ K. $n = 7$ is the maximal possible value

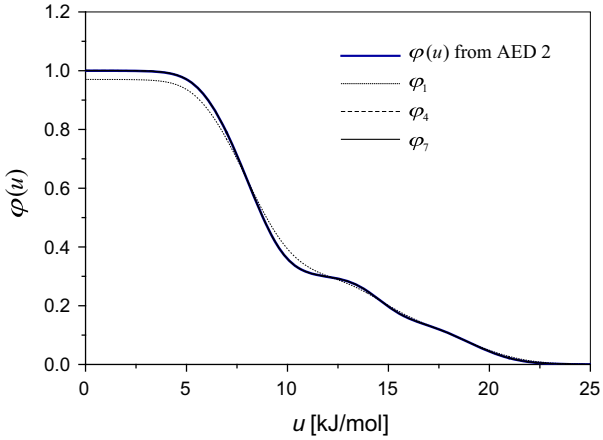

Fig. 6 Transformed total isotherms $\varphi_1,\ \varphi_4,\ \varphi_7$ and φ at $T = 77$ K corresponding to the adsorption energy distributions $F_1,\ F_4,\ F_7$ and AED 2 in Fig. 5

In Fig. 4 can be seen that F_4 really overlays the original distribution function AED 1, i.e. AED 1 is slightly better recalculated by means of (30) than by (28). The reason for this is that for every derivative of (30), the increment can be optimally chosen. In contrast to that, σ in (28) is a common parameter for all derivatives. This implies in general that the individual derivative is worse approximated. While the recalculated adsorption energy distributions obtained by (28) are non-negative, (30) produces small negative parts.

Also in the case of the more complicated distribution function AED 2, Eq. (30) shows a slightly better performance. However, the influence of F on its recalculation is shown by the fact that the approximation is not as good as for AED 1.

The instability of our problem is illustrated in Figure 6 by presenting the transformed total isotherms $\varphi_1,\ \varphi_4$ and φ_7 for the functions $F_1,\ F_4$ and F_7 of Fig. 5.

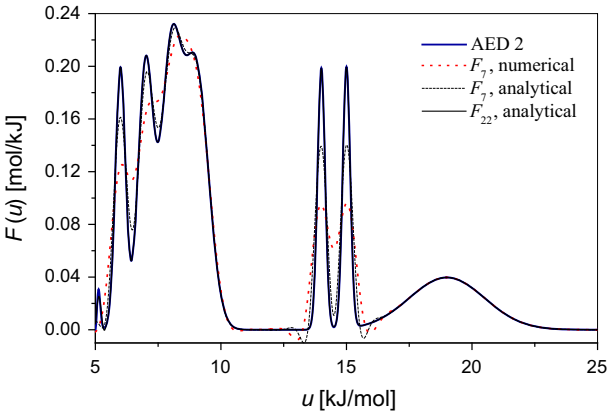

Fig. 7 Original synthetic AED 2 compared with analytical and numerical recalculations by means of (30)

From Fig. 6 it becomes obvious that φ_4, φ_7 and φ almost coincide although F_4, F_7 significantly differ from AED 2. Only φ_1 differ from φ because the distance between AED 2 and F_1 is large enough. Hence, the recalculation of AED 2 shows the limits of (28) and (30). In regions where the peaks are close together they cannot be resolved. The reason for that is the finite calculation accuracy. The round-off errors cause that:

- the increments for the higher derivatives in (30) increase,
- the amplification of the round-off errors by $\exp\left(\frac{(\pi RT)^2}{2\sigma^2}\right)$ in (28) becomes too large for small σ.

Hence, the higher derivatives are approximated with decreasing accuracy. The influence of the higher derivatives can be illustrated by using

$$\frac{1}{\pi RT}\sum_{l=0}^{n}\frac{(-1)^{l+1}(\pi RT)^{2l+1}}{(2l+1)!}\,\varphi^{(2l+1)} = \int_{u_{\min}}^{u_{\max}} F(v)\frac{1}{\pi RT}\sum_{l=0}^{n}\frac{(-1)^{l+1}(\pi RT)^{2l+1}}{(2l+1)!}\,k^{(2l+1)}(u-v)\,\mathrm{d}v \tag{31}$$

for the computation of F_n. The $k^{(2l+1)}$ can be computed analytically. Obviously, this method can be applied only for known F.

Figure 7 shows the comparison of the original AED 2 as given in Fig. 1 with analytical and numerical recalculations for $n = 7$ by means of (31) or (30), respectively. Additionally, the analytical recalculation for $n = 22$ is presented. The strong influence of round-off errors in the numerical approximation becomes obvious. The round-off errors lead to a decreasing accuracy of the higher derivatives that are needed for the resolution of peaks being located close together. Furthermore, it becomes obvious that analytically, (30) works very well.

4.2 Fourier series

Another possibility to recalculate F is developing F into an orthogonal series with respect to a complete orthonormal system. Since (19) is the basis of all inversion formulas and since trigonometric functions are Eigen functions of the differential operator, it is natural to use Fourier series.

For shortened notation we define

$$u^* := \frac{u_{\max} + u_{\min}}{2}, \qquad l := \frac{u_{\max} - u_{\min}}{2},$$
$$\mathrm{cs}_\kappa(u) := \cos\left(\frac{\kappa\pi(u-u^*)}{l}\right), \qquad \mathrm{sn}_\kappa(\mathrm{u}) := \sin\left(\frac{\kappa\pi(u-u^*)}{l}\right). \tag{32}$$

with (32), F can be presented by

$$F(u) = \frac{a_0}{2} + \sum_{\kappa=1}^{\infty}[a_\kappa \mathrm{cs}_\kappa(u) + b_\kappa \mathrm{sn}_\kappa(u)], \qquad u_{\min} \le u \le u_{\max} \tag{33}$$

with the Fourier coefficients

$$a_\kappa := \frac{1}{l}\int_{u_{\min}}^{u_{\max}} F(u)\mathrm{cs}_\kappa(u)\,\mathrm{d}u \quad \text{and} \quad b_\kappa := \frac{1}{l}\int_{u_{\min}}^{u_{\max}} F(u)\mathrm{sn}_\kappa(u)\,\mathrm{d}u, \qquad \kappa = 0, 1, 2, \ldots \tag{34}$$

(25) can be applied to the functions $p = \mathrm{cs}_\kappa$ or $p = \mathrm{sn}_\kappa$.

Using

$$P(u) = u \ \text{ for } \ p(u) = \mathrm{cs}_0(u), \qquad P(u) = \frac{l}{\kappa\pi}\mathrm{sn}_\kappa(u) \ \text{ for } \ p(u) = \mathrm{cs}_\kappa(u), \ \kappa > 0,$$
$$P(u) = -\frac{l}{\kappa\pi}\mathrm{cs}_\kappa(u) \ \text{ for } \ p(u) = \mathrm{sn}_\kappa(u), \ \kappa > 0$$

and

$$\begin{aligned}
&\mathrm{sn}_\kappa(u - i\pi RT) - \mathrm{sn}_\kappa(u + i\pi RT)\\
&= \frac{e^{i\frac{\kappa\pi(u-u^*)}{l}} e^{\frac{\kappa\pi^2 RT}{l}} - e^{-i\frac{\kappa\pi(u-u^*)}{l}} e^{-\frac{\kappa\pi^2 RT}{l}} - e^{i\frac{\kappa\pi(u-u^*)}{l}} e^{-\frac{\kappa\pi^2 RT}{l}} + e^{-i\frac{\kappa\pi(u-u^*)}{l}} e^{\frac{\kappa\pi^2 RT}{l}}}{2i}\\
&= \frac{2\mathrm{cs}_\kappa(u)\left[e^{\frac{\kappa\pi^2 RT}{l}} - e^{-\frac{\kappa\pi^2 RT}{l}}\right]}{2i} = -2i\sinh\left(\frac{\kappa\pi^2 RT}{l}\right)\mathrm{cs}_\kappa(u),
\end{aligned}$$

$$\begin{aligned}
&\mathrm{cs}_\kappa(u - i\pi RT) - \mathrm{cs}_\kappa(u + i\pi RT) \\
&= \frac{e^{i\frac{\kappa\pi(u-u^*)}{l}} e^{\frac{\kappa\pi^2 RT}{l}} + e^{-i\frac{\kappa\pi(u-u^*)}{l}} e^{-\frac{\kappa\pi^2 RT}{l}} - e^{i\frac{\kappa\pi(u-u^*)}{l}} e^{-\frac{\kappa\pi^2 RT}{l}} - e^{-i\frac{\kappa\pi(u-u^*)}{l}} e^{\frac{\kappa\pi^2 RT}{l}}}{2} \\
&= \frac{2i\,\mathrm{sn}_\kappa(t)\left[e^{\frac{\kappa\pi^2 RT}{l}} - e^{-\frac{\kappa\pi^2 RT}{l}}\right]}{2} = 2i\,\sinh\left(\frac{\kappa\pi^2 RT}{l}\right)\mathrm{sn}_\kappa(t),
\end{aligned}$$

we obtain

$$a_0 = -\frac{1}{l}\int_{-\infty}^{\infty}\varphi'(u)\,\mathrm{d}u, \quad a_\kappa = -\frac{\sinh\left(\frac{\kappa\pi^2 RT}{l}\right)}{\pi^2 RT\kappa}\int_{-\infty}^{\infty}\varphi'(u)\mathrm{cs}_\kappa(u)\mathrm{d}u, \quad \kappa > 0,$$

$$b_\kappa = -\frac{\sinh\left(\frac{\kappa\pi^2 RT}{l}\right)}{\pi^2 RT\kappa}\int_{-\infty}^{\infty}\varphi'(u)\mathrm{sn}_\kappa(u)\,\mathrm{d}u, \quad \kappa > 0.$$

Hence, F can be presented by

$$F(u) = -\frac{\alpha_0}{2l} - \frac{1}{\pi^2 RT}\sum_{\kappa=1}^{\infty}\frac{\sinh\left(\frac{\kappa\pi^2 RT}{l}\right)}{\kappa}\left[\alpha_\kappa \mathrm{cs}_\kappa(u) + \beta_\kappa \mathrm{sn}_\kappa(u)\right], \quad u_{\min} \le u \le u_{\max} \tag{35}$$

with

$$\alpha_\kappa := \int_{-\infty}^{\infty}\varphi'(u)\,\mathrm{cs}_\kappa(u)\,\mathrm{d}u, \quad \beta_\kappa := \int_{-\infty}^{\infty}\varphi'(u)\,\mathrm{sn}_\kappa(u)\,\mathrm{d}u, \quad \kappa \ge 0. \tag{36}$$

In analogy to (30), we define as approximations of F:[3]

$$\mathcal{F}_n(u) := -\frac{\alpha_0}{2l} - \frac{1}{\pi^2 RT}\sum_{\kappa=1}^{n}\frac{\sinh\left(\frac{\kappa\pi^2 RT}{l}\right)}{\kappa}\left[\alpha_\kappa\,\mathrm{cs}_\kappa(u) + \beta_\kappa\,\mathrm{sn}_\kappa(u)\right] \tag{37}$$

As can be seen in Fig. 8, (37) yields excellent results.

For $n = 6$, a perfect recalculation of AED 1 is obtained since the modulated Cosine we use is a fourier sum consisting of seven terms. For a perfect recalculation of AED 2 (sum of Gaussians), all terms of the fourier series are needed. Numerically, fourty nine terms ($n = 48$) are satisfying. It becomes clear that (37) with $n = 48$ yields much better results than the best approximation by means of (30).

In (37), explicit terms for error amplification are given. An error in the coefficient α_κ or β_κ, resp., will be amplified by the factor $\frac{\sinh\left(\frac{\kappa\pi^2 RT}{l}\right)}{\pi^2 RT\kappa}$. This allows the quantitative

[3] In order to distinguish this approximation by the approximation F_n given in (43), we choose the symbol $\mathcal{F}_n$.

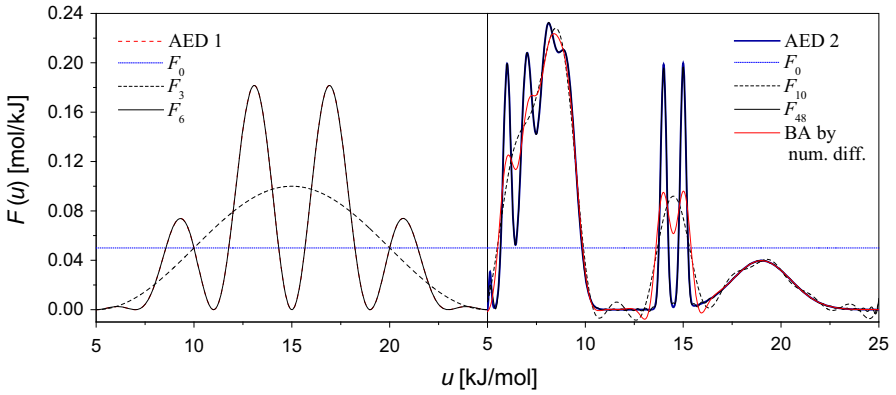

Fig. 8 *Left* Recalculation of AED 1 by (37) for $n = 0$, $n = 3$, $n = 6$ and $T = 77$ K. *Right* Recalculation of AED 2 by (37) for $n = 0$, $n = 10$, $n = 48$ and $T = 77$ K in comparison with the best approximation (BA) by (30)

estimation of the instability of the adsorption integral equation with Langmuir kernel and shows that the problem is severely instable.

The quality of approximation by finite Fourier sums depends on the smoothness of F. If F is m-times continuously differentiable with periodic boundary conditions, then α_k and β_κ behave like $\alpha_\kappa, \beta_\kappa = o\left(\kappa^{-m}\right)$. Hereby, cut-off criteria for the sum in (37) can be derived.

In summary, approximation (37) offers the following advantages:

1. Very good recalculations can be obtained also for complicated adsorption energy distributions (cf. Fig. 8).
2. Explicit and simple terms for error amplification exist.
3. Cut-off criteria can be derived.

Taking into account these advantages, (37) makes a good candidate as a basis for a regularization scheme.

5 The influence of temperature on the stability of the solution

Considering (28), (30) and (37) it becomes obvious that the quality of recalculation of F depends on temperature. Therefore, we will investigate the behavior of (7) for low and high temperatures, i.e. the transformed total isotherm is considered as a function of ζ and T : $\varphi = \varphi(\zeta, T)$.

The terms for error amplification decrease in amplitude as temperature decreases. In (28) and (37), they approximate the limits

$$\lim_{T\to 0} \exp\left(\frac{(\pi RT)^2}{2\sigma^2}\right) \frac{\sin\left(\frac{\pi RT(u-v)}{\sigma^2}\right)}{\pi RT} = \frac{u-v}{\sigma^2} \quad \text{and} \quad \lim_{T\to 0} \frac{1}{\pi^2 RT} \frac{\sinh\left(\frac{\kappa\pi^2 RT}{l}\right)}{\kappa} = \frac{1}{l}. \tag{38}$$

Equation (38) indicates that for $T \to 0$, it holds:

$$F(u) = -\lim_{T \downarrow 0} \varphi'(u, T), \qquad u_{\min} < u < u_{\max}. \tag{39}$$

By estimating $|\varphi'(u, T) + F(u)|$ quantitatively, we can show that (39) is valid. For that, F is supposed to be continuously differentiable. With $I = [u_{\min}, u_{\max}]$, one obtains:

$$|\varphi'(u, T) + F(u)| = \left| \varphi'(u, T) + F(u_{\max}) - \int_u^{u_{\max}} F'(v) \mathrm{d}v \right| \tag{40}$$

$$\leq \frac{F(u_{\max}) \exp\left(\frac{u-u_{\max}}{RT}\right)}{1 + \exp\left(\frac{u-u_{\max}}{RT}\right)} + \frac{F(u_{\min})}{1 + \exp\left(\frac{u-u_{\min}}{RT}\right)}$$

$$+ \left| \int_{u_{\min}}^{u} \frac{F'(v)}{1 + \exp\left(\frac{u-v}{RT}\right)} \mathrm{d}v - \int_u^{u_{\max}} \frac{F'(v) \exp\left(\frac{u-v}{RT}\right)}{1 + \exp\left(\frac{u-v}{RT}\right)} \mathrm{d}v \right|$$

$$\leq \frac{F(u_{\max}) \exp\left(\frac{u-u_{\max}}{RT}\right)}{1 + \exp\left(\frac{u-u_{\max}}{RT}\right)} + \frac{F(u_{\min})}{1 + \exp\left(\frac{u-u_{\min}}{RT}\right)} \tag{40.1}$$

$$+ \left\| F' \right\|_{\infty, I} \left[u - u_{\min} - RT \ln\left(1 + \exp\left(\frac{u - u_{\min}}{RT}\right)\right)\right] \tag{40.2}$$

$$+ \left\| F' \right\|_{\infty, I} RT \left[2 \ln 2 - \ln\left(1 + \exp\left(\frac{u - u_{\max}}{RT}\right)\right)\right]. \tag{40.3}$$

All three terms (40.1)–(40.3) converge to 0 for $T \to 0$ and $u_{\min} < u < u_{\max}$. (40.1) and (40.2) are only significant in the neighborhood of $u_{\min}$ and $u_{\max}$. The quality of convergence depends mainly on (40.3), i.e. $|\varphi'(u, T) + F(u)|$ converges at least linearly, and the speed of convergence is determined by the maximal absolute value of the derivative of F. A similar computation shows that $\frac{F(u)}{2} = -\lim_{T \downarrow 0} \varphi'(u, T)$ holds at $u = u_{\min}, u_{\max}$. The convergence is also dominated by $\left\| F' \right\|_{\infty, I} RT$.

Notice that the situation in the neighborhood of $u_{\min}$ and $u_{\max}$ is symmetric. This can be seen if $\left| \varphi'(u, T) + F(u_{\min}) + \int_{u_{\min}}^{u} F'(v) \ \mathrm{d}v \right|$ is chosen as the right-hand side of (40). Better estimates on the quality of convergence in (39) are obtained by considering the second derivative of F.

Equations (40.1)–(40.3) show quantitatively that the quality of the recalculation of F depends on F itself or more precisely on special properties of F. By means of AED 2, we illustrate the influence of lowering temperature on the recalculation of F using the first derivative of φ.

Figure 9 shows how the transformed total isotherm φ change with temperature.

With decreasing temperature, the steps in the transformed total isotherm become more pronounced. This illustrates that with decreasing temperature, the peaks in the underlying AED will be resolved better by the first derivative of the transformed total isotherm (cf. Fig. 10).

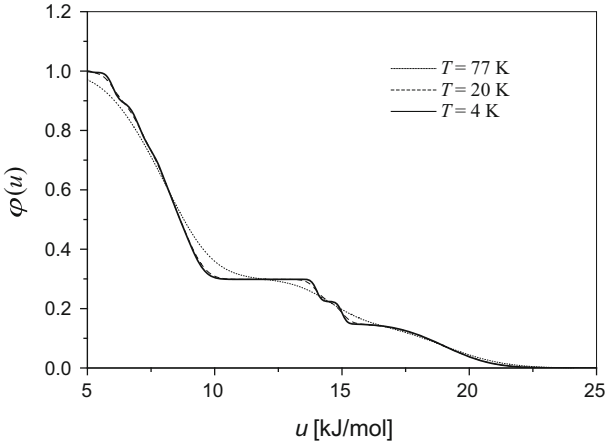

Fig. 9 Transformed total isotherm φ belonging to AED 2 for three temperatures

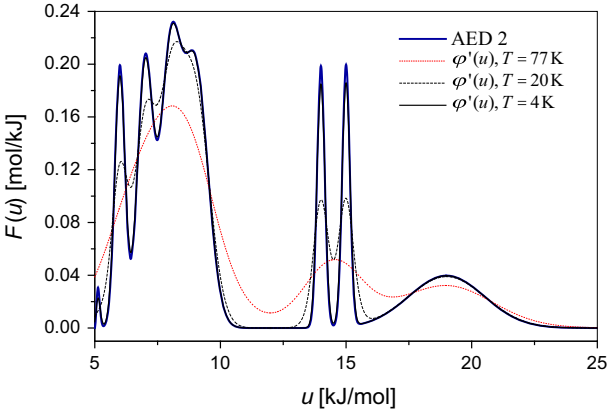

Fig. 10 Original synthetic AED 2 compared with recalculations from the transformed total isotherms in Fig. 9 by means of the first derivative for three temperatures

Additionally, it is shown that the approximation of F by $-\varphi'$ depends locally on the maximum of $|F'|$. The reason for that is that the kernel function k (cf. (17)) and its derivative localize around 0. Hence $k(u - \cdot)$ or $k'(u - \cdot)$, resp., localize around u. Therefore, $\|F'\|_{\infty,I}$ in (40.2) and (40.3) can be replaced by $\|F'\|_{\infty,[u-\varepsilon,u+\varepsilon]}$ for suitable ε depending on temperature T without making a significant error.

Since F in Fig. 10 has zero boundary values, i.e. $F(u_{\min}) = F(u_{\max}) = 0$, the term (40.1) is also zero. The term (40.2) is only significant in the neighborhood of $u_{\min}$.

If one considers high temperatures, it holds uniformly on any interval:

$$\lim_{T\to\infty} \varphi(\zeta, T) = \int_{u_{\min}}^{u_{\max}} \frac{F(u)}{2}\,\mathrm{d}u = \frac{1}{2}$$

Hence for $T \to \infty$, we have the worst case of non-uniqueness, and every AED produces the same total isotherm. Therefore, a numerical recalculation of AEDs will be more difficult with increasing temperature.

6 Conclusions

In this paper, a solution theory has been established for the adsorption integral equation with Langmuir kernel by deriving complex and real inversion formulas. This theory allows the calculation of adsorption energy distributions from transformed total adsorption isotherms.

The first result of our work is that in general only regularization methods lead to stable solutions. Only if the set of possible adsorption energy distributions is strongly restricted, also analytical methods can be applied.

The main results are the following:

1. By means of inversion formulas it is shown how the fourier coefficients of the adsorption energy distribution can be computed by integrals over the transformed total isotherm. This allows the recalculation of adsorption energy distributions by fourier series.
2. In the error-free case, the fourier series approach works very well also for complicated adsorption energy distributions. In the erroneous case, moreover, the error of any fourier coefficient can be calculated explicitly by the error of the total isotherm, i.e. explicit and simple terms for error amplification exist. For this reasons, the fourier series approach makes a good candidate as a basis of a regularization scheme.
3. For low temperatures, the derived real inversion formula as infinite sum of derivatives of the transformed total isotherm is also a good choice for recalculating adsorption energy distributions. As lower the temperature the better the first term of this sum approximates the adsorption energy distribution. Therefore, higher order terms can be neglected. This shows that lowering the temperature stabilizes the solution.

We can conclude that the first step of a promising regularization scheme for the adsorption integral equation with Langmuir kernel is done, i.e. a family of regularization operators with the property of pointwise convergence [cf. (3)] has been constructed by (30) or (37).

Acknowledgments The financial support for this project by Deutsche Forschungsgemeinschaft (DFG, KA 1560/6-1) is gratefully acknowledged.

Compliance with Ethical Standards

Conflict of interest The authors declare that they have no conflict of interest.

References

1. M. Jaroniec, P. Bräuer, Surf. Sci. Rep. **6**, 65 (1986)
2. M. Jaroniec, R. Madey, *Physical Adsorption on Heterogeneous Solids* (Elsevier, Amsterdam, 1988)
3. W. Rudzinski, D.H. Everett, *Adsorption of Gases on Heterogeneous Surfaces* (Academic Press, London, 1992)
4. M.V. Szombathely, P. Bräuer, M. Jaroniec, J. Comput. Chem. **13**, 17 (1992)
5. P. Bräuer, M. Fassler, M. Jaroniec, Thin Solid Films **123**, 245 (1985)
6. R. Kress, *Linear Integral Equations* (Springer, Berlin, 1989)
7. S. Arnrich, G. Kalies, P. Bräuer, Appl. Surf. Sci. **268**, 5198 (2010)
8. S. Arnrich, G. Kalies, P. Bräuer, Adsorption **17**, 823 (2011)
9. C.W. Groetsch, *Stable Approximate Evaluation of Unbounded Operators* (Springer, Berlin, 2007)
10. A. Rieder, *Keine Probleme Mit Inversen Problemen* (Vieweg & Sohn, Wiesbaden, 2003)
11. H.W. Engl, M. Hanke, A. Neubauer, *Regularization of Inverse Problems* (Springer, Dordrecht, 2000)
12. J. Hadamard, *Lectures on Cauchy's Problem in Linear Partial Differential Equations* (Yale University Press, New Haven, 1923)
13. D. Widder, *The Stieltjes Transform* (American Mathematical Society, Harvard University, 1938). http://www.ams.org/journals/tran/1938-043-01/S0002-9947-1938-1501933-2/S0002-9947-1938-1501933-2.pdf. Assessed 20 June 2014
14. J. Elstrodt, *Maß- und Integrationstheorie* (Springer, Berlin, 1996)
15. R. Paley, N. Wiener, *Fourier Transforms in the Complex Domain*, vol. 19 (American Mathematical Society Colloquium Publications, American Mathematical Society, Providence, RI, 1987), pp. x+184. Reprint of the 1934 original